Organic versus Hybrid Coacervate Complexes : Co-Assembly and Adsorption Properties

J. Fresnais[*], J.-F. Berret[*], L. Qi[**], J.-P. Chapel[**], J.-C. Castaing[**]

[*] : Matière et Systèmes Complexes, UMR 7057 CNRS Université Denis Diderot Paris-VII, Bâtiment Condorcet, 10 rue Alice Domon et Léonie Duquet, 75205 Paris, France
[**] Complex Fluid Laboratory, UMR CNRS/Rhodia 166, Rhodia North-America, R&D Headquarters CRTB, 350 George Patterson Blvd., Bristol, PA 19007 USA

ABSTRACT

We report the co-assembly and adsorption properties of coacervate complexes made from polyelectrolyte-neutral block copolymers and oppositely charged cerium oxide nanoparticles. We first show that the electrostatic complexation resulted in the formation of stable core-shell aggregates in the 100 nm range. The microstructure of the CeO_2-based complexes was resolved using cryogenic transmission electronic microscopy, which revealed that the cores were clusters made from densely packed nanoparticles. The adsorption properties of the same complexes were investigated by stagnation point adsorption reflectometry. The adsorbed amount was measured as a function of time for polymers and complexes using anionically charged silica and hydrophobic poly(styrene) substrates. It was found that all complexes adsorbed readily on both types of substrates up to a level of 1 – 2 mg m^{-2} at stationary state. Upon rinsing however, the adsorbed layer was not removed. Combining the efficient adsorption and strong stability of the CeO_2–based core-shell hybrids on various substrates, it is suggested that these systems could be used appropriately for coating and anti-biofouling applications.

Keywords: *nanoceria – colloidal complexes – block copolymers - SPAR*

1 INTRODUCTION

In the context of electrostatic complexation, it has been shown that polyelectrolyte-neutral copolymers exhibited interesting clustering and coating properties. These hydrosoluble macromolecules were found to co-assemble with oppositely charged systems, e.g. with surfactants [1-3], polymers [4-8] and proteins [9,10], yielding "supermicellar" aggregates with core-shell structures. As a result, the core of the aggregates was described as a dense coacervate microphase comprising the oppositely charged species. Made from neutral blocks, the corona was identified as surrounding the cores and related to the stability of the whole colloid. In the present paper, the same type of formulations were conducted 7 nm cerium oxide nanoparticles (CeO_2, nanoceria). Nanoceria were considered because of their potential applications in catalysis [11,12], polishing and coating technologies [13] as well as in biology [14,15]. The main goal of the present survey was to search for synergistic complexation effects in the context of coating and anti-biofouling applications. Cohen Stuart and coworkers have shown that electrostatic complexes made from oppositely charged polyelectrolytes could be efficiently adsorbed on charged hydrophilic and on hydrophobic surfaces, such as silica and poly(styrene) respectively [6,7,16]. These authors have also demonstrated the stability of the deposited layer upon rinsing, and its remarkable anti-fouling properties with addition of proteins [6,7,16]. The approach followed here has consisted to extend the adsorption measurements to new types of electrostatic complexes, namely to complexes built from anionically-coated cerium oxide nanoparticles and cationic-neutral block copolymers [17,18].

2 EXPERIMENTAL

For the electrostatic complexation, we have used poly(trimethylammonium ethylacrylate methylsulfate-b-poly(acrylamide) block copolymer, hereafter noted $PTEA_{11K}$-*b*-PAM_{30K} and cerium oxide nanocrystals. Light scattering performed in the dilute regime of concentrations have revealed hydrodynamic diameter D_H = 11 nm and 8.6 nm, respectively [19]. Cryo-TEM images of single nanoparticles are displayed in Fig. 1a. An image analysis has allowed us to determine the size distribution function which was log-normal with median diameter D = 6.9 ± 0.3 nm and polydispersity s = 0.15. Nanoceria were coated by PAA_{2K} using the precipitation-redispersion pathway recently described in the literature. Quantitative determinations using small-angle scattering experiments and chemical analysis have disclosed a brush comprising ~ 50 PAA_{2K} chains adsorbed at the interfaces [20]. A cryo-TEM image of the PAA_{2K}-coated nanoceria is displayed in Fig. 1b. This technique revealed isolated particles with size and size distribution identical to those obtained for the bare acidic particles. Mixed solutions of nanocolloids and copolymers were prepared by simple one-shot mixing of

NSTI-Nanotech 2008, www.nsti.org, ISBN 978-1-4200-8503-7 Vol. 1

dilute solutions prepared at the same concentration c (c ~ 1 wt. %) and same pH .

The amount of adsorbed polymers and coacervates deposited onto silica or poly(styrene) (PS) surfaces was monitored using Stagnation Point Adsorption Reflectometry (SPAR) [21]. Fixed angle reflectometry measured the reflectance at the Brewster angle on the flat substrate. A linearly polarized light beam was reflected by the surface and subsequently splitted into a parallel and a perpendicular component using a polarizing beam splitter. As material adsorbed at the substrate-solution interface, the ratio S between the parallel and perpendicular components of the reflected light varied. The system was analyzed in terms of Fresnel reflectivities for a multi-layer system (substrate, coating, adsorbed layer and solvent), where each layer was described by a complex refractive index and a layer thickness. At the stagnation point the hydrodynamic flow was zero leading to diffusion-limited exchanges between the injected solution and the collecting surface.

Hydrophilic silica substrates were modeled using smooth silicon wafers covered with a layer of ~ 100 nm SiO_2. Hydrophobic poly(styrene) substrate was modeled by a poly(styrene) thin layer of ~ 100 nm deposited on top of an HMDS (hexamethyldisilizane) functionalized silicon wafer by spin-coating a toluene solution (2.5 wt. %) at 5000 rpm.

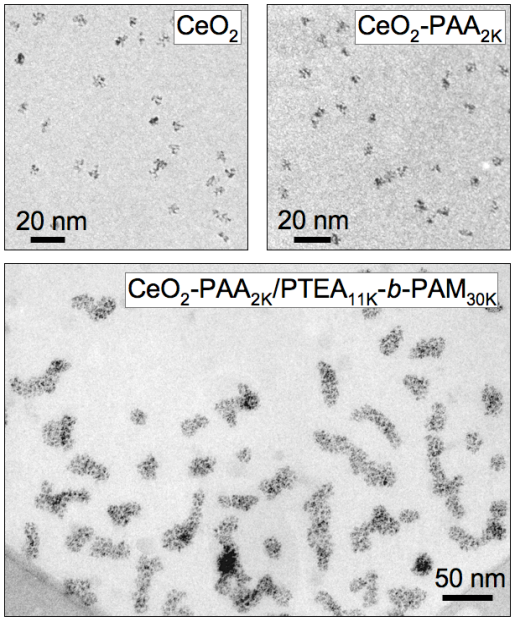

Figure 1 : Cryogenic transmission electron microscopy (cryo-TEM) images of bare and coated cerium oxide nanoparticles. Upper left panel : bare CeO_2 in acidic conditions (pH 1.4); Upper right panel : CeO_2 coated with poly(acrylic acid) with molecular weight 2000 g mol^{-1} (pH 8). Lower panel : CeO_2-PAA_{2K} complexed with the oppositely charged diblock copolymers $PTEA_{11K}$-*b*-PAM_{30K}.

3 RESULTS

3.1 Cryo-TEM

Cryo-TEM was also performed on CeO_2-PAA_{2K}/$PTEA_{11K}$-*b*-PAM_{30K} dilute sample, and an illustration of the hybrid aggregates is provided in Fig. 1c (lower panel). The photograph covers spatial field that is 0.36×0.50 μm^2 and displays clusters of nanoparticles [19]. A large visual field was shown here in order to stress that the clusters were dispersed in solutions, a result which was consistent with the visual observations of the solutions. A closer inspection revealed that the aggregates were slightly anisotropic, with a fixed diameter around 20 nm and slight polydispersity in length and morphology. Elongated and branched aggregates were observed too in Fig. 1c, with length comprised between 20 and 100 nm [18].

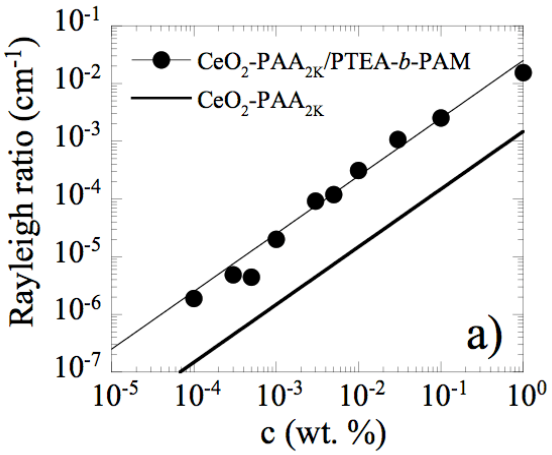

Figure 2 : Concentration dependences of the Rayleigh ratios obtained by light scattering (in the 90°-configuration) for CeO_2-PAA_{2K}/$PTEA_{11K}$-*b*-PAM_{30K}. The thick straight lines depict the intensities calculated assuming that nanoparticles and polymers were not associated.

3.2 Critical Association Concentration

Fig. 2 show the concentration dependences of the Rayleigh ratio for CeO_2-PAA_{2K}/$PTEA_{11K}$-*b*-PAM_{30K} formulated at c = 1 wt. %. A linear variation was found down to a concentration of 10^{-4} wt. %. Contrary to the data of the organic complexes [17,18], Fig. 2 did not exhibit a drop of the intensity upon dilution. For this sample, dynamic light scattering has revealed a slightly polydisperse diffusive relaxation mode associated with hydrodynamic diameters D_H = 100 ± 10 nm. In Fig. 2, the scattering intensities obtained from unassociated nanoparticles and polymers were shown for comparison (thick line). The observation of a linear dependence down to the lowest concentration available, and well above the

unassociated state supports the assumption that the hybrids are stable toward dilution, and that their critical association concentration is below 10^{-4} wt. %. For the organic complexes discussed in Refs. [17,18], the critical association concentration was of the order of 10^{-2} wt. %.

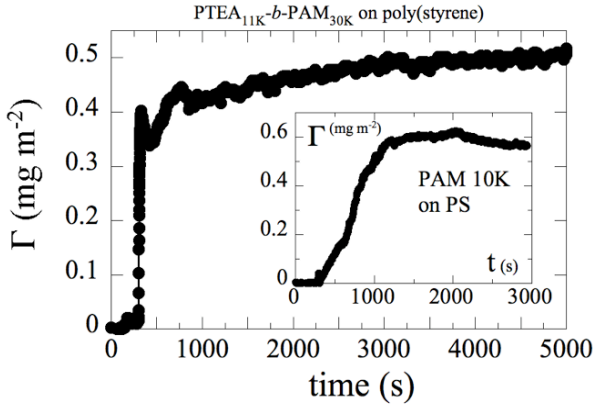

Figure 3 : Adsorption kinetics for $PTEA_{11K}$-*b*-PAM_{30K} block copolymers on poly(styrene) substrate as received from stagnation point adsorption reflectometry. Measurements were performed with dilute solutions at c = 0.1 wt. %. Inset : adsorption kinetics for poly(acrylamide) molecular weight 10 000 g mol^{-1} operated in the same conditions. In both experiments, rinsing with de-ionized water did not remove the polymer layer.

3.3 Adsorption kinetics for polymers

Adsorption kinetics was first monitored on silica and poly(styrene) model substrates using $PTEA_{11K}$-*b*-PAM_{30K} polymeric solutions. In dilute solutions, the copolymers are considered as dispersed and non-aggregated. On anionically charged silica surfaces, $PTEA_{11K}$-*b*-PAM_{30K} were found to adsorb up to a value of Γ_{ST} = 0.8 mg m^{-2}. This adsorption was most likely due to the electrostatic attractive interactions between the opposite charges coming from the cationic polyelectrolyte blocks and the surface. A subsequent rinsing with de-ionized water did not remove the copolymer layer. In the case of a hydrophobic PS surfaces, adsorption was found at a lower level however than on silica surfaces (Γ_{ST} = 0.4 - 0.6 mg m^{-2}). This is a surprising result since in the case a strong polyelectrolyte on an uncharged surface, electrostatics is not expected to contribute to the adsorption energy. In order to understand this phenomenon, reflectometry was also carried out in the same conditions on the different homopolymers with comparable molecular weights, namely PTEA and PAM [18]. On hydrophobic PS surfaces, poly(acrylamide) with molecular weight 10 000 g mol^{-1} was the only polymer to adsorb spontaneously at a low but significant level (Γ_{ST} = 0.5 mg m^{-2}, inset in Fig. 3). Again, in this particular case no desorption occurred on rinsing. One possible explanation is the release of water molecules trapped in a frozen-like structure close to the hydrophobic surface [7].

3.4 Adsorption kinetics for Hybrid Coacervates

Figs. 4 show the adsorption properties of the hybrid coacervates CeO_2-PAA_{2K}/$PTEA_{11K}$-*b*-PAM_{30K} on silica and on PS substrates. The two sets of data exhibit the same behavior : after an adsorption process at a level 0.8 – 1.4 mg m^{-2}, no desorption occurred upon rinsing. We explain the absence of desorption observed here as a consequence of the strong stability of the polymer-particle hybrids upon dilution, a result that was already emphasized in a previous report, and also by light scattering. Clearly, the existence of a very low critical aggregation concentration for the particle-polymer hybrids (below 10^{-4} wt. %) guarantees the integrity of the deposited layer on the two substrates [17,18].

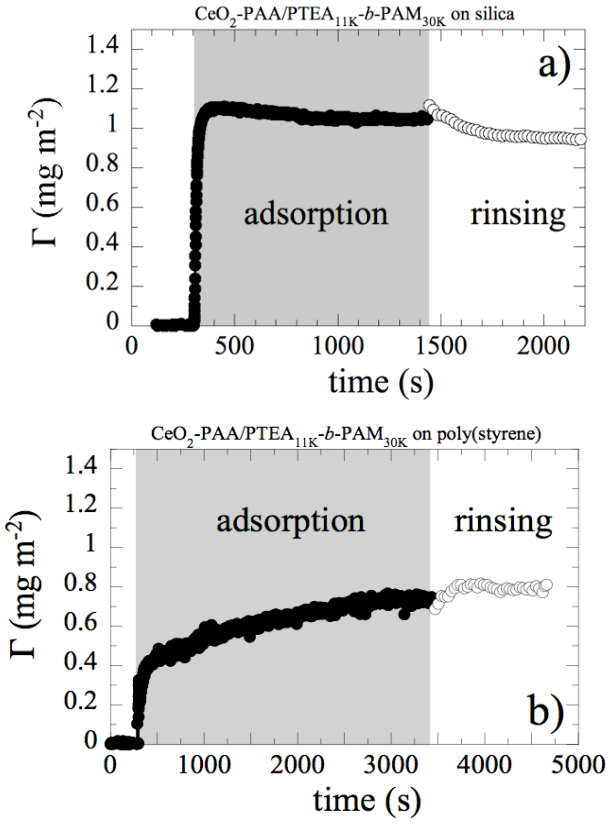

Figure 4 : Adsorption kinetics for organic core-shell SDS/$PTEA_{11K}$-*b*-PAM_{30K} coacervates complexes on a) anionically charged silica and b) hydrophobic poly(styrene) substrate. Upon rinsing, the reflectometry signal dropped down to a level comprised between 0.3 – 0.5 mg m^{-2}. The decrease of the reflectometry signal suggests that the adsorbed layer has been partially removed during this second phase.

NSTI-Nanotech 2008, www.nsti.org, ISBN 978-1-4200-8503-7 Vol. 1

4 CONCLUSION

We have investigated the bulk and surface properties of mixed aggregates resulting from the co-assembly between cerium oxide nanoparticles and block copolymers. Cryo-TEM observations have disclosed unambiguously the cluster-like microstructure of the hybrid aggregates. These results compare very well to those found recently on oxide nanoparticles coated with citrates counterions [19]. The SPAR measurements have shown that organic and hybrid aggregates adsorbed readily on model substrates. At steady state, the adsorbed amount attained values of the order of 1 – 1.5 mg m^2, which correspond to a single and densely packed monolayer of colloids. SPAR experiments were also performed with the copolymers alone, as well as with the homopolymers from which these copolymers were composed. From these tests, it was recognized that poly(acrylamide) with molecular weight 10 K adsorbed spontaneously on PS, a result that was not reported for this substrate. This latter findings was important since it allowed us to conclude that the adsorption of the coacervates was primarily driven by that of the PAM corona.

REFERENCES

[1] T.K. Bronich; T. Cherry; S. Vinogradov; A. Eisenberg; V.A. Kabanov; A.V. Kabanov. Langmuir 14 (1998) 6101.

[2] P. Hervé; M. Destarac; J.-F. Berret; J. Lal; J. Oberdisse; I. Grillo. Europhys. Lett. 58 (2002) 912 .

[3] J.-F. Berret; P. Hervé; O. Aguerre-Chariol; J. Oberdisse. J. Phys. Chem. B 107 (2003) 8111 .

[4] M.A.C. Stuart; N.A.M. Besseling; R.G. Fokkink. Langmuir 14 (1998) 6846 .

[5] A. Harada; K. Kataoka. Science 283 (1999) 65 .

[6] S.v.d. Burgh; A.d. Keizer; M.A.C. Stuart. Langmuir 20 (2004) 1073 .

[7] S.v.d. Burgh; R. Fokkink; A.d. Keizer; M.A.C. Stuart. Colloids and Surfaces A - physicochemical and Engineering Aspects 242 (2004) 167 .

[8] B. Hofs; A. deKeizer; M.A. CohenStuart. J. Phys. Chem. B 111 (2007) 5621 .

[9] F. Cousin; J. Gummel; D. Ung; F. Boue. Langmuir 21 (2005) 9675 .

[10] M. Danial; H.-A. Klok; W. Norde; M.A. CohenStuart. Langmuir 23 (2007) 8003 .

[11] M. Nabavi; O. Spalla; B. Cabane. J. Colloid Interface Sci. 160 (1993) 459 .

[12] M. Das; S. Patil; N. Bhargava; J.-F. Kang; L.M. Riedel; S. Seal; J.J. Hickman. Biomaterials 28 (2007) 1918 .

[13] X. Feng; D.C. Sayle; Z.L. Wang; M.S. Paras; B. Santora; A.C. Sutorik; T.X.T. Sayle; Y. Yang; Y. Ding; X. Wang; Y.-S. Her. Science 312 (2006) 1504 .

[14] R.W. Tarnuzzer; J. Colon; S. Patil; S. Seal. Nano Lett. 5 (2005) 2573 .

[15] J. Chen; S. Patil; S. Seal; J.F. McGinnis. Nature Nanotechnology 1 (2006) 142 .

[16] M.A.C. Stuart; B. Hofs; I.K. Voets; A.d. Keizer. Curr. Opin. Colloid Interface Sci. 10 (2005) 30 .

[17] L. Qi; J.P. Chapel; J.C. Castaing; J. Fresnais; J.-F. Berret. Langmuir 23 (2007) 11996.

[18] L. Qi; J.P. Chapel; J.C. Castaing; J. Fresnais; J.-F. Berret. Soft Matter 4 (2008) 577 – 585.

[19] J.-F. Berret; A. Sehgal; M. Morvan; O. Sandre; A. Vacher; M. Airiau. J. Colloid Interface Sci. 303 (2006) 315 .

[20] A. Sehgal; Y. Lalatonne; J.-F. Berret; M. Morvan. Langmuir 21 (2005) 9359 .

[21] G.J. Fleer; M.A. Cohen Stuart; J.M.H.M. Scheutjens; T. Cosgrove; B. Vincent. Polymers at Interfaces; Chapman & Hall: London, 1993.